1949

Analysis of a double skin and corrugated thin flat plate.

Irgens, Donald Leroy

University of Michigan

Minneapolis, Minnesota
July 15, 1949

Faculty Committee
Department of Aeronautical Engineering
University of Minnesota
Minneapolis, Minnesota

Sirs:

Enclosed herewith is completed thesis submitted to you for approval.

Subject thesis is for partial fulfillment of the requirements for a degree of Master of Science in Aeronautical Engineering.

ANALYSIS OF A

DOUBLE SKIN AND CORRUGATED

THIN FLAT PLATE

by

eroy

Donald L. Irgens

July 15, 1949

TABLE OF CONTENTS

SUMMARY

An experimental investigation was made on the behavior of a test panel constructed of 0.025 aluminum corrugation with 0.032 aluminum skin on both sides. Such a panel was subjected to a compressive load in the longitudinal direction with the unloaded edges simply supported. The panel was long in reference to its width.

Tests showed that inter-rivet buckling induced by inferior blind riveting or too large a rivet spacing would precipitate early panel failure before actual critical load would occur, on a well designed panel.

Such type of construction proved very stable up to loads approaching the critical value. The strength weight ratio indicated it to be very desirable in aircraft construction.

An analytical analysis was made using both non-isotropic and isotropic plate theory; both methods predicted the critical load to within 7.5 per cent of each other, thus indicating that the double skin and corrugation type plate, of the design under consideration, acts much like an isotropic plate.

Because of the fact that such a plate will buckle at a load that will induce strains in the sheet and corrugation above their elastic limits, it was necessary,

in the analytical analysis, to use reduced values for the modulus of elasticity. The prediction of the behavior of the metal in the plastic range is not exact thus indicating such a prediction as critical load is difficult for this type construction.

In the analytical analysis, we use computed values for the modulus of elasticity. The penetration of the behavior of the mold in the plastic range is not exact thus introducing such a prediction as additional load is difficult for this type construction.

INTRODUCTION

The problem under consideration in this report was to study the behavior of a plate of the double skin corrugation construction when subjected to a compression load. Special emphasis was given to the determination of the critical buckling load.

A considerable amount of research work on this type of construction has been carried out by the Glenn L. Martin Aircraft Factory, but considering the complexities that arise in the analysis of any non-isotropic plate, additional research work on it seemed warranted.

The analysis was limited to aluminum alloy plates so designed that the initial buckling stress of the skin and the crippling stress of the corrugation were approximately equal so as to eliminate skin buckling before panel failure.

The experimental tests were limited to a plate loaded with a uniform axial load parallel to the sides of the plate; the unloaded edges were simply supported.

The thesis work was done by the writer during the school year 1948-49 at the University of Minnesota. Thesis advisor was Professor Joseph A. Wise.

EQUIPMENT AND PROCEDURE

Test Specimen.

The details of the test panel are shown on Fig. 2. The material for the panel was furnished by the Glenn L. Martin Aircraft Factory, fabrication of the plate was by the writer.

As noted in Fig. 2 the panel is tapered in plan-form and thickness, the original plans for the investigation called for a non-tapered section but due to non-availability of desired material the plate was constructed as shown. It was felt that the small amount of taper did not materially change the conditions that would be found in a non-tapered section. For conservatism the minimum section was used for the analytical analysis.

Internal strain gauges with necessary leads were placed before fabrication of cover skins. All strain gauges were placed in duplicate at locations as shown on Fig. 2.

Filler blocks along supported sides so designed to separate skins along supports proved very successful in providing a symmetric support.

Filler blocks at top and bottom of plate designed primarily to transmit the load to the corrugation, were found unnecessary and were removed after initial test.

Principal Apparatus.

The principal apparatus required for the tests was a suitable jig to support the panel simply along the two unloaded edges; a further non-functional requirement was to make the jig simple and light enough for one man to handle. Such a jig was designed, details of which are shown on Fig. 4.

A 400,000 pound capacity Tinus Olsen testing machine was used for subject tests. The width of the swivel head of the machine corresponded to the width of the top of the panel.

Minor Apparatus.

The leads from the strain gauges were soldered into a junction box made up with Mallory infant jacks; connections from junction box to Baldwin and Southwark "K" box was by electrical phone plugs.

Procedure.

The general procedure of the tests was to load the plate by increments, then take strain and deflection readings. It was found that for the load that was placed on the plate during the tests no appreciable deflection was observed, an indication that such type construction is very stable up to critical load.

Three separate tests were made, results of which are shown graphically in Figs. 6 to 14 and in tabular form on Tables I to III.

Tests are described separately below giving details of each.

Test I.

Load increments of 6,000 pounds were applied; at panel load of 23,000 pounds local failure occurred at top of panel. Upon investigation of local failure it was found that edge supports did not run up high enough, giving an unsupported section of 2 inches at top of plate. Corrective measure taken was to remove the upper 1½ inches of plate, giving only a ½ inch unsupported plate for test number two.

Test II.

Load increments of 6,000 pounds were applied with one intermediate panel load of 19,850 pounds. Panel load went up to 30,000 pounds at which point local failure occurred at bottom of panel. Upon investigation of local failure it was found that the filler block on bottom did not transmit the load properly to the corrugation and caused a local failure in bearing of the corrugation. This was corrected by trimming 2½ inches from the bottom and removing filler block.

Test III.

Load increments of 12,000 pounds were applied up to 24,000 pounds, plate remained stable up to 30,000

pounds at which point readings were recorded. Upon increasing the load to 31,600 pounds a failure occurred at approximately 12 inches from the top of the panel. The failure at first appeared to be the critical load for the panel but upon examination of failure it was observed that at point of failure, on one of the cover sheets, one horizontal row of rivets had pulled out thus subjecting the skin to twice its original unsupported length, this reduced the critical buckling stress of the sheet to a point which precipitated the failure.

Above plate load of 30,000 pounds it was observed that inter-rivet buckling had started.

Upon reaching the load where one row of rivets pulled out it appeared as though plate had started to form 3 definite half waves of approximately equal length, the loading was not continued however since another test was to be run on the undamaged remainder.

Test IV.

Plate was trimmed to a 56 inch length. Load increments were applied similar to those in test three.

Inter-rivet buckling was observed to start at panel load of 31,000 pounds. One definite half wave formed in the longitudinal direction at a load of 34,000 pounds at which point severe inter-rivet buckling occurred on one plate, while other plate remained flat. Maximum deflection of half wave was at center of plate and was estimated

to be one and one half inches, since deflection was greater than Ames dial capacity at that point.

RESULTS AND DISCUSSION

Load, strain data is presented on Tables I-IV. The principal strains were obtained from rosette readings by method described in Reference 2 of bibliography. Plots of principal stresses versus plate loads are shown on Figs. 5-14.

It was unfortunate that none of the four tests produced a true critical load on the plate, however, it was felt that the tests proved successful as they clearly showed the stability of this type construction in the region of design load. The indications of the tests were such that the panel would be well in its plastic range before the critical load would be reached; a theoretical analysis, which will be presented subsequently, bears this fact out quite clearly.

Inasmuch as the critical load on a panel such as this is of no practical value, it is used extensively as a design criteria, that is by being able to predict what the critical load is and knowing the behavior of the plate up to critical, a safe design load may be arrived at.

The tests bore out the fact that any rivet failure will induce early skin instability, it appeared that had the rivet spacing been decreased to three fourths of an inch, the skin would have remained stable and

probably would have allowed the plate to reach a full critical value.

Theoretical Analysis.

The method used in the theoretical analysis follows quite closely the work as presented in Reference 1.

The critical load on a non-isotropic plate similarly loaded and supported to the one of this test is given in Reference 3 as:

$$P_{CR} = \frac{2\pi^2}{b^2} \sqrt{(D_x)(D_y)} + D_3$$

where: P_{CR} = critical load in pounds per unit width

b = plate width, small in reference to length

D_x = average flexural rigidity per unit width of the plate parallel to the y axis

D_y = same as D_x but parallel to x axis

$D_3 = \frac{1}{2}\left[\mu D_y + \mu D_x\right] + 2(GI)_{xy}$

$2(GI)_{xy}$ = average torsional rigidity of the plate (ratio of the moment per unit width to the twist)

also: $D_x = \frac{(EI)_x}{1 - \mu_x\mu_y}$, $D_y = \frac{(EI)_y}{1 - \mu_x\mu_y}$

Since flexural rigidity about an axis parallel to y is contributed to by both sheet and corrugation, and about an axis parallel to x is contributed mainly by sheet, D_x and D_y are conservatively written as:

$$D_x = \frac{(E_{sheet} I_{sheet})_x}{1 - \mu^2} + (E_{corr} I_{corr})_x$$

$$D_y = \frac{(E_s I_s)_x}{1 - \mu^2}$$

For further conservatism effect of corrugation in D_x is omitted in evaluation of D_3, hence:

$$D_3 = \frac{(E_s I_s)_x}{1 - \mu^2} + 2(GI)_{xy}$$

In Reference 1 it is shown that the term $2(GI)_{xy}$ is a constant and can be replaced by $G_e t_s d^2$, where:

G_e = effective shear modulus

t_s = bare skin thickness

d = distance between skins

Tests conducted on corrugation columns at the Glenn L. Martin Company indicate that the tangent modulus of elasticity of the compression stress strain curve can be used to predict the value of E_c for the type plate in question, hence Fig. 18 was plotted from properties as given in Fig. 17.

$(E_s)_x$ is also taken as the tangent modulus of the average strain strain curve from the properties of flat sheet when the critical buckling load has been exceeded. Such a curve is plotted on Fig. 20 from data of Fig. 19. For conservatism $(E_s)_y$ has been taken as equal to $(E_s)_x$.

Effective shear modulus has been studied quite extensively for this type construction in Reference 1,

and a value of 0.7 G has proved to be quite reliable for cases of the plate being stressed above the elastic limit.

By assuming a series of maximum strains and calculating P_{CR} by the non-isotropic plate equation just given, then finding corresponding load a stable plate will carry at similar strains by $P'_{CR} = \sigma_{corr}A_{corr} + \sigma_{sheet}A_{sheet}$ and plotting results, the intersection of two plots will give predicted critical load for panel; such a plot is given on Fig. 21. A typical calculation for making the graph is given under Sample Calculations of this thesis.

The predicted critical load was determined to be 2,900 pounds per inch of width; for an average width of 17 inches between supports this would correspond to a total panel load of 49,300 pounds. Maximum strain in plate at critical load was predicted at 0.00345 inches per inch.

This theoretical analysis indicates the plate goes well into the plastic range of the material before critical load is obtained. In reference to actual test results it can be readily seen that plate was obeying Hooke's Law almost up to the point where local skin buckling precipitated panel failure, and that if skin had not buckled prematurally load could have continued up to near predicted critical.

CONCLUSIONS

Corrugation and double skin type of construction forms a very stable panel and maintains this stability very close to its critical load. The strength weight ratio is very high, a factor of significance in aircraft construction.

Relating the test results to theoretical calculations indicates that a design load critical load ratio is in the neighborhood of 0.6.

The need for precise riveting and rigid inspection after completing a panel seems very necessary since panels of this type depend largely on the flexural rigidity contributed by the sheets, for stability.

The test results did not indicate a true critical load, however had inter-rivet buckling been suppressed by a more precise rivet job or a decreased rivet spacing it is believed the actual and predicted critical load would have approached each other.

The analytical analysis is by no means an exact one, since various assumptions as to the behavior of the plate in the plastic range have been made, however it appears quite reliable in reference to repeated applications by the Glenn L. Martin Aircraft Company.

The plate apparently can be treated as an isotropic plate based on the analysis of an isotropic plate by

the method of strain energy, as given in Appendix A. The analysis as given in Appendix A predicts a critical load about 7.5 per cent higher than by analyzing the plate as being non-isotropic.

BIBLIOGRAPHY

1. Kennedy, W. B., Troxell, W. W.: Study of Compression Panel Supported on Four Edges, Formed of Corrugated Sheet with Flat Skin on Both Sides. Structural Development Report 21, Glenn L. Martin Company, 1944.

2. Wise, Joseph A.: Circles of Strain. Journal of the Aeronautical Sciences, Vol. 7, No. 10, pp. 438-40, August 1940.

3. Timoshenko, S.: Theory of Elastic Stability, McGraw-Hill Book Company, 1936.

SAMPLE CALCULATIONS

For: $P_{cr} = \frac{2\pi^2}{b^2}\left[\sqrt{(D_x)(D_y)} + D_3\right]$ Ref. page Fig. 21

$P'_{cr} = \sigma_{Corr.} A_{corr} + \sigma_{sheet\,(Ave.)} A_{sheet}$

[illegible]: $\epsilon_{[illegible]} = 0.0038$ in/in

[illegible]. $G_c = \frac{[illegible] E}{2(1+\mu)} = (0.7[illegible])E$

[illegible] below [illegible] limit

$I_s = 0.[illegible]5475$ in.^{4}/in, $A_s = 0.[illegible]4$ in^2/in

$I_c = 0.0[illegible]59$ in.^{4}/in, $A_c = 0.0375$ in^2/in

$d = [illegible]25$ in. [illegible], distance between skins

$t_s = 0.0272$ in. {[illegible] 0.032 Alum.}

$t_c = 0.0[illegible]22$ in {bare 0.[illegible]5 Alum.}

$b = 1[illegible]$ in. {[illegible] width of plate}

$\mu = 0.3$ $(1-\mu^2) = 0.91$

$\frac{2\pi^2}{b^2} = 0.05716$, E_t [illegible] see Fig. 20, t_c see Fig. 18

$G t_s$ [illegible] $= 49,[illegible]00$, σ_{Corr} see Fig. 19, σ_{sheet} see Fig. 19

$\therefore$ $D_x = \frac{E_t I_s}{1-\mu^2} = \frac{1.6\times10^6 \times .00[illegible]5475}{0.91} + 7.4\times10^6 \times .00[illegible]$

$= 1[illegible]25 + 11,750 = [illegible],375$ [illegible]

$D_y = [illegible]25$ [illegible] in., $D_3 = [illegible]([illegible]) + 0.7([illegible]) = 31,4[illegible]$

$P_{cr} = .05716\left[10^6\sqrt{(.02[illegible])([illegible]62)} + 31,445\right]$

$P_{cr} = [illegible]$ lbs/in.

[illegible]

$P'_{cr} = (3[illegible],[illegible]00)(.0375) + (2[illegible],[illegible]00)(.0[illegible]) = 3138$ lbs/in

SAMPLE CALCULATIONS (Con't)

Reduction of 45° strain rosette data to principal strains. (Ref. 2)

Test #1 Load = 13,000# Table #I

Sheet #1 45° Rosette 36 in from top.

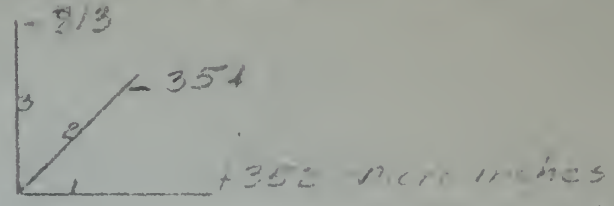

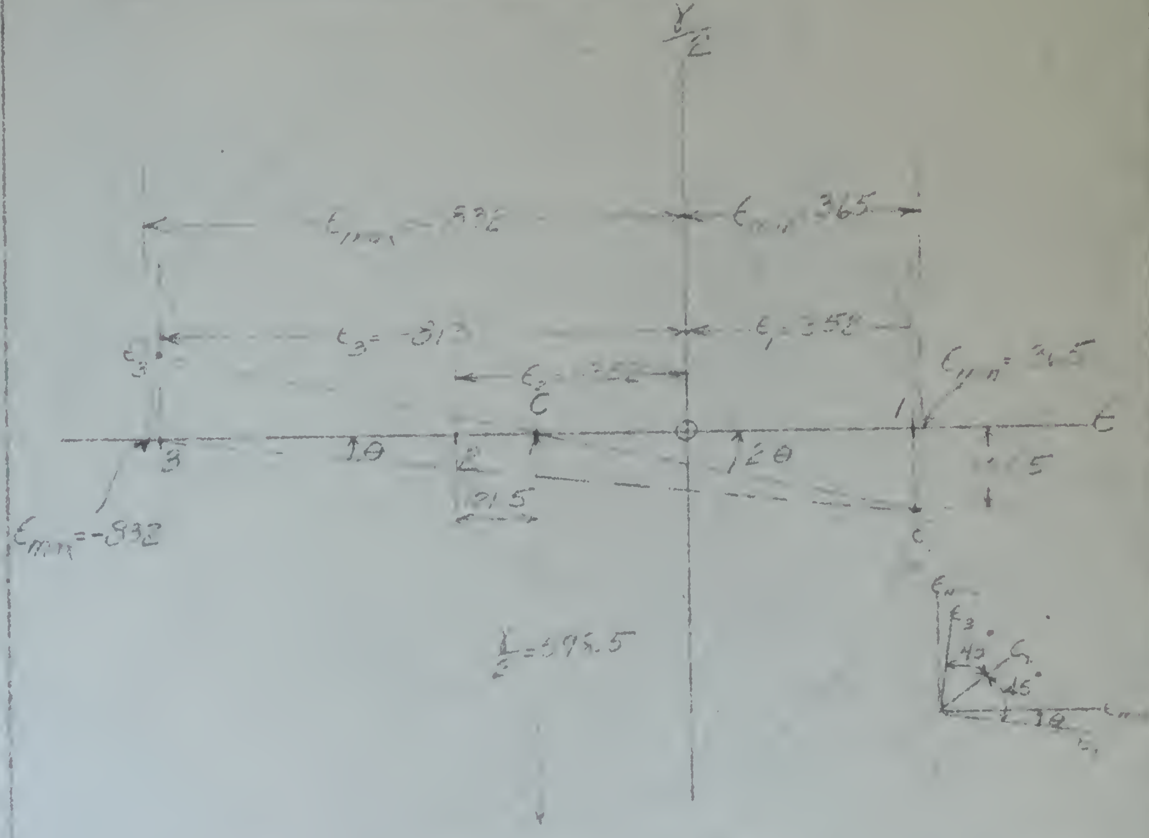

C is mid point between 1 and 3 [illegible]

$$\sigma_{max} = \frac{E}{1-\mu^2}\left[\epsilon_{max} + \mu\epsilon_{min}\right], \quad \sigma_{min} = \frac{E}{1-\mu^2}\left[\epsilon_{min} + \mu\epsilon_{max}\right]$$

Appendix A

Comparison of stability criteria applied to the isotropic plate analysis.

Isotropic analysis by method of strain energy.

General expression for internal strain energy.

$U_i = \int \frac{1}{2}\sigma\epsilon\, dV$

By assuming a configuration for a deflection curve, an expression expressing the internal and external strain energy can be worked out.

∴ Assume loading, deflection and configuration of isotropic plate to be as shown below:

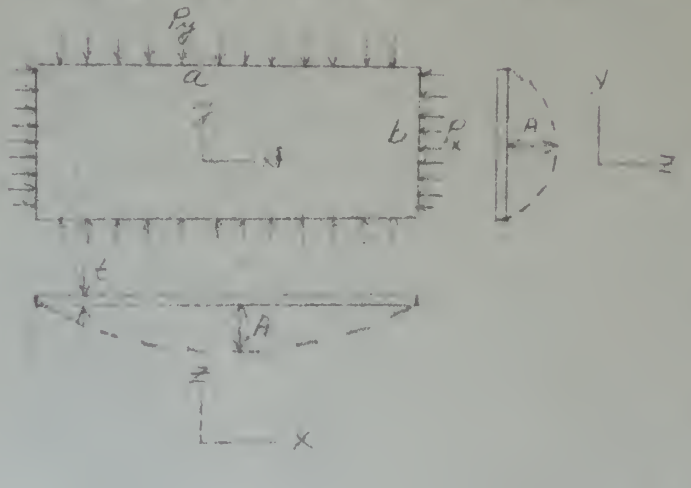

Assume m [illegible]

$w = A \sin\frac{m\pi x}{a} \sin\frac{n\pi y}{b}$

Where: A = max. defl.

m = Number of half sin waves in x dir.

n = Number of half sin waves in y dir.

(sketch shows m = n = 1)

By expressing stresses and strains in terms of deflection curve as shown:

$$\sigma_x = \frac{E}{1-\mu^2}\, z \left[\frac{\partial^2 w}{\partial x^2} + \mu \frac{\partial^2 w}{\partial y^2}\right]$$

$$\epsilon_x = z \frac{\partial^2 w}{\partial x^2}$$

$$\sigma_y = \frac{E}{1-\mu^2}\, z\left[\frac{\partial^2 w}{\partial y^2} + \mu\frac{\partial^2 w}{\partial x^2}\right]$$

$$\epsilon_y = z\,\frac{\partial^2 w}{\partial y^2}$$

$$\tau_{xy} = G\gamma_{xy} = \frac{E}{2(1+\mu)}\cdot 2z\,\frac{\partial^2 w}{\partial x\,\partial y}$$

$$\gamma_{xy} = 2z\,\frac{\partial^2 w}{\partial x\,\partial y}$$

Expression for internal strain energy becomes:

$$U_i = \frac{1}{2}\int_{-t/2}^{t/2}\left[\frac{Ez^2}{1-\mu^2}\left\{\left(\frac{\partial^2 w}{\partial x^2}\right)^2 + 2\mu\frac{\partial^2 w}{\partial x^2}\frac{\partial^2 w}{\partial y^2} + \left(\frac{\partial^2 w}{\partial y^2}\right)^2\right\} + \frac{2Ez^2}{2(1+\mu)}\left(\frac{\partial^2 w}{\partial x\,\partial y}\right)^2\right]dz$$

Since $\int_{-t/2}^{t/2} z^2\,dz$ is [illegible] equal to I expression reduces to:

$$U_i = \frac{EI}{2(1-\mu^2)}\iint\left[\left(\frac{\partial^2 w}{\partial x^2}\right)^2 + \left(\frac{\partial^2 w}{\partial y^2}\right)^2 + 2\mu\frac{\partial^2 w}{\partial x^2}\frac{\partial^2 w}{\partial y^2} + 2(1-\mu)\left(\frac{\partial^2 w}{\partial x\,\partial y}\right)^2\right]dx\,dy$$

For expression for external work [illegible]

$U_e = \frac{1}{2}\int w\,q\,dA$ where dA is [illegible]

$\therefore\ \Pi = U_{int} - U_{ext}$

$\therefore\ U_{int}$ [illegible]

By expansion in binomial theorem

$$L_c = \int_0^l \left[1 + \frac{1}{2}\left(\frac{\partial y}{\partial x}\right)^2 + \ldots\right] dx$$

$$\therefore \delta l = L_c - L_{ax} = \frac{1}{2}\int \left(\frac{\partial y}{\partial x}\right)^2$$

$$\therefore V_2 = \frac{1}{2}\int P \left(\frac{\partial w}{\partial x}\right)^2 dx$$

For given case

$$\int \left(\frac{\partial^2 w}{\partial x^2}\right)^2 dA = \frac{m^4 \pi^4 f^2 b}{4 a^3}$$

$$\int \left(\frac{\partial^2 w}{\partial y^2}\right)^2 dA = \frac{n^4 \pi^4 f^2 a}{4 b^3}$$

$$\int \left(\frac{\partial^2 w}{\partial x^2} \cdot \frac{\partial^2 w}{\partial y^2}\right) dA = \frac{m^2 n^2 \pi^4 f^2}{4ab}$$

$$\int \left(\frac{\partial^2 w}{\partial x \partial y}\right)^2 dA = \frac{m^2 n^2 \pi^4 f^2}{4ab}$$

$$\therefore V_1 = \frac{EI}{2(1-\mu^2)}\left[\frac{\pi^4 f^2}{4a^3b^3}\right]\left[m^4 b^4 + n^4 a^4 + 2\mu(m^2 n^2 a^2 b^2) + 2(1-\mu)(m^2 n^2 a^2 b^2)\right]$$

or

$$V_1 = \frac{EI}{2(1-\mu^2)} \frac{\pi^4 f^2}{4a^3b^3}\left[(m^2 b^2 + n^2 a^2)^2\right]$$

and

$$V_2 = \int \frac{P_x}{2} \frac{m^2 \pi^2 f^2}{a^2} \cos^2 \frac{m\pi x}{a} \sin^2 \frac{n\pi y}{b} \, dA + \int \frac{P_y}{2} \frac{n^2 \pi^2 f^2}{b^2} \sin^2 \frac{m\pi x}{a} \cos^2 \frac{n\pi y}{b} \, dA$$

or $V_2 = \frac{1}{2} A^2 \pi^2 \left[\frac{F_x m^2 b}{4a} + \frac{F_y n^2 a}{4b} \right]$

then equate $V_1 = V_2$ for equilibrium of plate, this gives:

$$\left[F_x m^2 b^2 + F_y n^2 a^2 \right] = \frac{E I}{(1-\mu^2)} \frac{\pi^2}{a^2 b^2} \left(m^2 b^2 + n^2 a^2 \right)^2$$

For conditions of test $F_y = 0$

Since the double skin and corrugation type plate will not buckle before reaching the elastic limit of the material it is necessary to use a reduced modulus in predicting a critical load. The method used in arriving at effective values of E in the non-isotropic analysis will be used here.

By assuming various combinations of half waves in above developed equation the minimum F loading thus obtained will be the critical loading of the plate. The wave formation in the short direction for such a case can be proven to be always of $n = \frac{1}{2}$ wave.

[illegible]

[illegible] (See Fig. 18)

[illegible] 17)

[illegible] 20

[illegible] 19)

[illegible]

Therefore it is apparent that plate would take the form of five or six half-waves in the long direction (and 1 in short direction)

[illegible] minimum as [illegible] came [illegible] orthotropic theory to check [illegible] result [illegible]

$K_c' = [illegible]$

$\therefore$ of [illegible] conditions

$P_{cr} = (38,000)(0.075) + (26,300)([illegible]) = [illegible]$ k/in

For any given plate the procedure should be to assume various maximum strains at which plate would reach critical load, at these strains obtain Effective Modulus of Elasticity of corrugation and sheet and corresponding stresses in the materials at assumed strains. Plot up results similarly to that of Fig 21 which will produce critical load of plate.

From above isotropic analysis the

Predicted critical load for plate was 3120 lbs/in. whereas non-isotropic plate theory gives a value of 2800 pounds per inch of width. The difference is relatively small which indicates the plate acts much as an isotropic plate. The slightly higher value obtained using the isotropic plate theory was mainly due to the fact that the flexural rigidity of the plate was due to both the sheet and corrugation about both the x and y axis, whereas in the non-isotropic theory, the contribution of the corrugation to the flexural rigidity about an axis parallel to the corrugation was omitted.

Fig. 2

Diagram of Test Panel

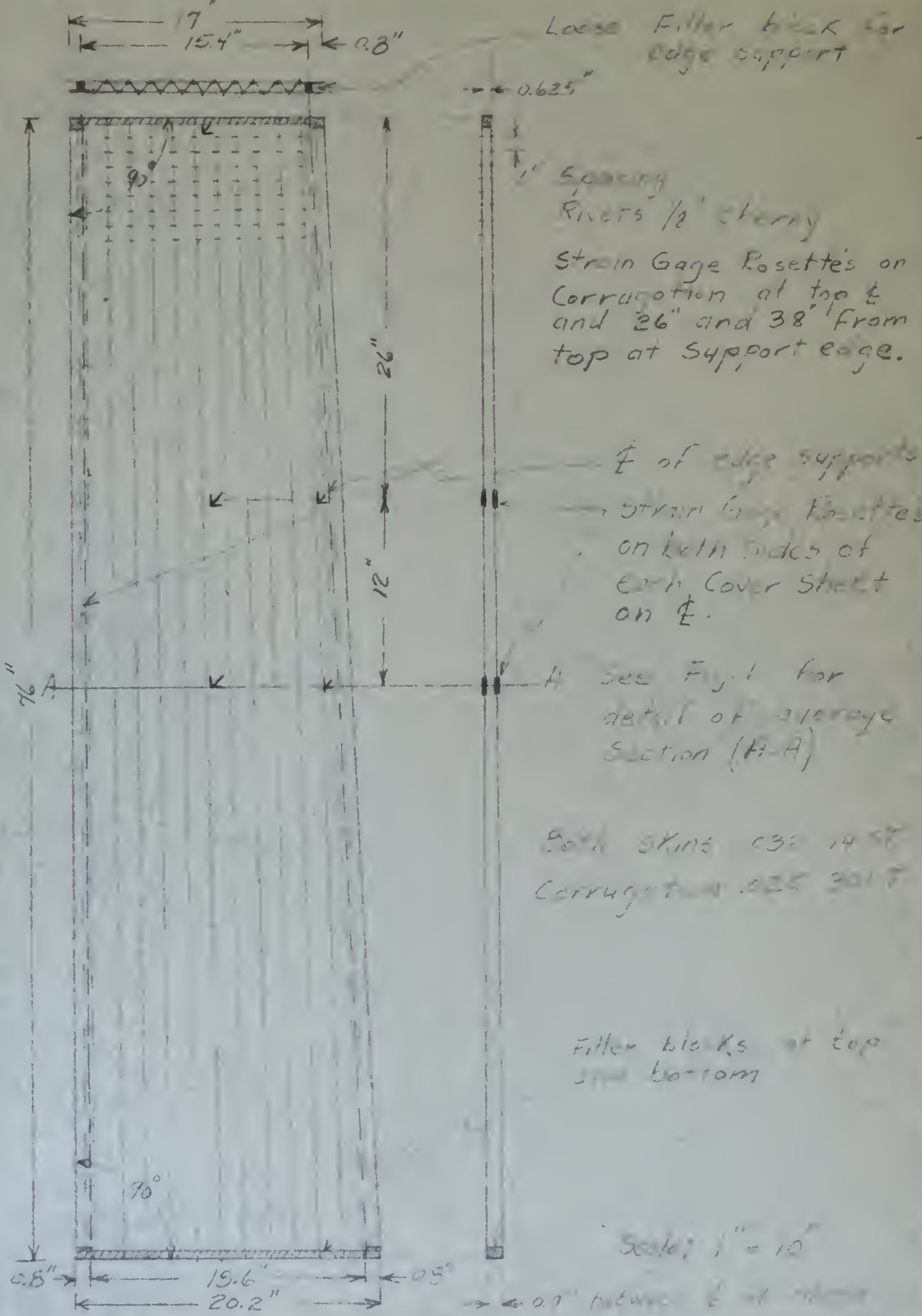

Fig. 3

Panel Loading Diagram

<u>Note</u>

Edges simply supported for support detail see Fig. 4.

Uniform compression Load in x direction.
Zero load in y direction.
Zero load in z direction.
x dimension is large with respect to y.

Fig. 4

Diagram of Testing Jig

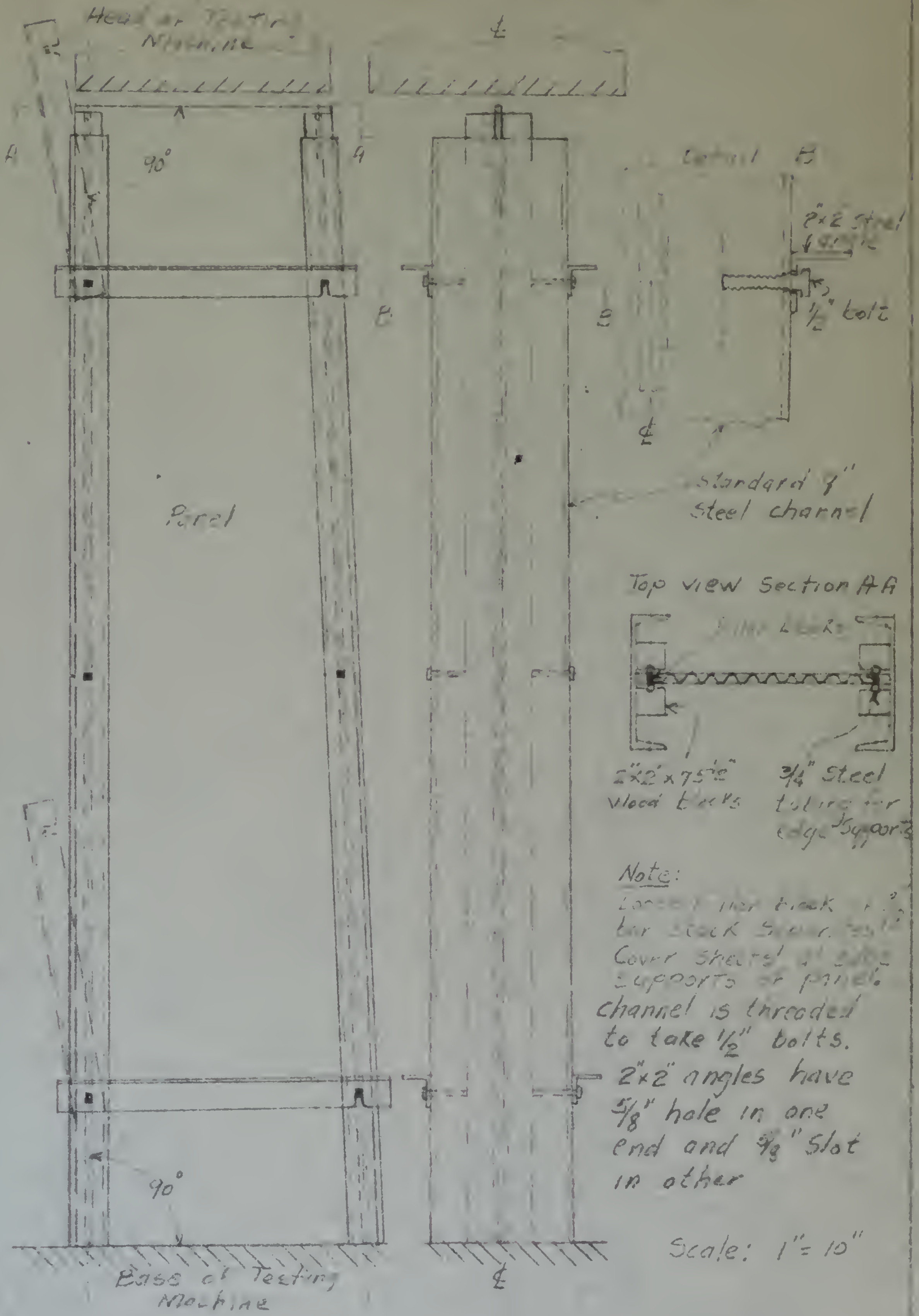

Table I

Test #1

$\mu = 0.3$, $E = 10^7$

Plotted on Figs 5-6-7

Gage location	Gage No.	Panel load 6000 lbs. Strain Micro inches	Stress lbs/in²	Shear lbs/in²	Panel load 12,000 lbs. Strain	Stress	Shear	Panel load 18,000 lbs. Strain	Stress	Shear
Plate 1										
38 in from top on ℄ Vert	18-25-	-281			-540			-813		
" Horz	19-26-	+121			+250			+352		
" 45°	21-28-	-132			-235			-354		
Principal		-240	-2160		-550	[illegible]		-832	-7?35	
		+130	+473	1616	+260	+1045	[illegible]	+365	+1270	4693
Plate 2										
26 in. from top on ℄ Vert	1-8-	-260			-544			-753		
" Horiz	2-9	+79			+132			+204		
" 45°	3-10-	-131			-235			-25?		
Principal		-265	-2635		-506	-5120		-762	-7670	
		+85	+60	1347	+135	-165	2427	+214	-161	3754
38" from top on ℄ Vert	4-	-235			-490			-741		
" Horiz	5-12-	+56			+162			+262		
" 45°	7-14-	-135			-240			-340		
Principal		-243	[illegible]		-491	-4530		-750	-7350	
		+63	-110	1177	+172	+272	2551	+270	+605	3977
Corrugation										
26 in. from top on edge Vert	37-44-	-96			-360			-544		
" Horiz	38-45	+61			+132			+191		
" 45°	39-46	-65			-130			-200		
Principal		[illegible]	-775		-362	-3596		-545	-5350	
		+75	+465	708	+134	+279	1907	+192	+313	2832
38 in. from top on edge Vert	40-47	-208			-466			-611		
" Horiz	41-48-	+75			+159			+235		
" 45°	42-50-	-74			-151			-245		
Principal		-211	-2030		[illegible]	[illegible]		-615	-5970	
		+88	+272	1151	+160	-717	2184	+240	+605	3287

[illegible] ... [illegible]

Plate 1																
3-1 in from [illegible] Top c. £ Vert	1, 20	750			-515			770			-815			-1025		
" Horiz	19	+125			+[illegible]			+33[illegible]			-344			+182		
" 45°	3/21	135			-205			-339			-355			-397		
Principal		-261 -250			[illegible] -4440			-[illegible] -151		1206	-540 -7[illegible]			-1034 -1705		
		+134	+[illegible]	1577	+28	+37	3/[illegible]	+[illegible]	+1697	4678	+40	1112	4105	+775	+1982	5346
Plate 2																
34½ in from top on £ Vert	1, 3	-253			-415			-774			-854			-179		
" Horiz	2	+81			+22[illegible]			+29[illegible]			+[illegible]			+749		
" 45°	[illegible]	-70			-168			-250			-280			-345		
Principal		-255 -250			-406 -475			-774 -1785			-855 -8110			-1050 -10,49		
		+[illegible]	+605	[illegible]	+201	+617	2641	+798	+158	4177	+361	+15	4650	+730	+[illegible]7	5578
36½ in from top on £ Vert	4, 5	22[illegible]														
" Horiz		+77														
" 45°	7, 14	[illegible]														
Principal		-[illegible] -384			-477 [illegible]			-70[illegible] -[illegible]			-354 -[illegible]5			-1046 -[illegible]		
		+[illegible]	+77	1516	+136	+[illegible]	[illegible]	+[illegible]	+[illegible]	4[illegible]	[illegible]	+1256	4115	+[illegible]	+41	5[illegible]
[illegible] from top [illegible] Vert	37, 64	166			-357			-548			-660			-8[illegible]		
" Horiz	38, 4, 2.7	[illegible]			+160			+225			+260			+310		
" 45°	4[illegible]	-4[illegible]			-1[illegible]			-182			-230			-270		
Principal		-167	-[illegible]		-[illegible]	-[illegible]		-541	-5[illegible]		-661	-1400		-[illegible]	[illegible]	
		+70	+219	71	+118	+123	1822	+226	+[illegible]	2[illegible]	+161	+88	3[illegible]41	+4[illegible]	-[illegible]	4[illegible]
[illegible] from top [illegible] edge Vert	[illegible], 47	-117			-45[illegible]			-670			-786			-910		
" Horiz	4, 48	+[illegible]			+1[illegible]			+160			+225			+310		
" 45°	5[illegible], 50	[illegible]			-12[illegible]			-200			-235			-280		
Principal		-1[illegible]	-1970		-4[illegible]	-460		-[illegible]	-[illegible]		-758	7700		-[illegible]	-[illegible]	
		+[illegible]	-[illegible]	54[illegible]	+[illegible]	-225	3[illegible]	+164	-417	3221	+227	-1035	3437	+[illegible]	+41[illegible]	[illegible]

Table [illegible] [illegible]

[illegible] Extension [illegible]

Location of Gage	Gage No.	[illegible] lbs. Strain	Stress	Shear	[illegible] lbs. Strain	Stress	Shear	[illegible] lbs. Strain	Stress	Shear
Plate 1										
36½ in from top on ℄ Vert	16 25	-628			1278			-1695		
" Horiz	2 22	+270			+516			+600		
" 45°	21 28	-250			-520			-840		
Principal		-632	-6040		-1290	-12,430		-1740	-17,000	
		+274	+927	3484	+523	+1484	6962	+640	+1297	9148
Plate 2										
34½ in from top on ℄ Vert	1 8	-494			-930			-1015		
" Horiz	2 9	+202			+410			+540		
" 45°	3 10	-175			-350			-330		
Principal		-500	-4820		-940	-8950		-1023	-9430	
		+205	+605	2762	+420	+1517	5238	+550	+2560	5995
36½' from top on ℄ Vert	4 11	-475			-985					
" Horiz	6 13	+208			+455					
" 45°	7 14	-178			-399					
Principal		-480	-4570		-1000	-9575		-1180	-10910	
		+213	+751	2664	+461	+1770	5672	+631	+3045	6978
Corrugation 36½" from top on edge Vert	40 47	-519			1040			-1320		
" Horiz	41 48	+175			+310			+480		
" 45°	43 50	-135			-340			-440		
Principal		-522	-5150		-1042	-10430		-1321	-12,820	
		+177	+224	2687	+311	-44	5198	+481	+932	6876

[illegible]

Table IV

Test # 1 Plates on Fig. 14

Gage location	Gage No.	Frame load 12,000 lbs: Strain micro-in. per in.	Stress lb/in²	Shear lb/in²	Case load [illegible] lbs: Strain	Stress	Shear	Panel load [illegible] lbs: Strain	Stress	Shear
Plate 1										
12 in. from top on ℄ Vert	25-	-570			-1160					
" Horiz	2-	+200			+730					
" 45°	18-	-345			-500					
Principal		-590 +212	-5300 +1581	2094	-1170 +410					
Compression 12 in. from [illegible] on edge Vert		-630 +155			-1190 -345			-432 +553		
" Horiz	5-	-70			-360			-500		
" 45°		-640 +160	[illegible] 355	2824	-1191 +346	[illegible] -124	[illegible]	-532 +550	[illegible] [illegible]	[illegible]
Principal										

Fig. 5

Plate Load vs. Max. Cover Sheet(1) Stress
(Test #1)
Re: Table II

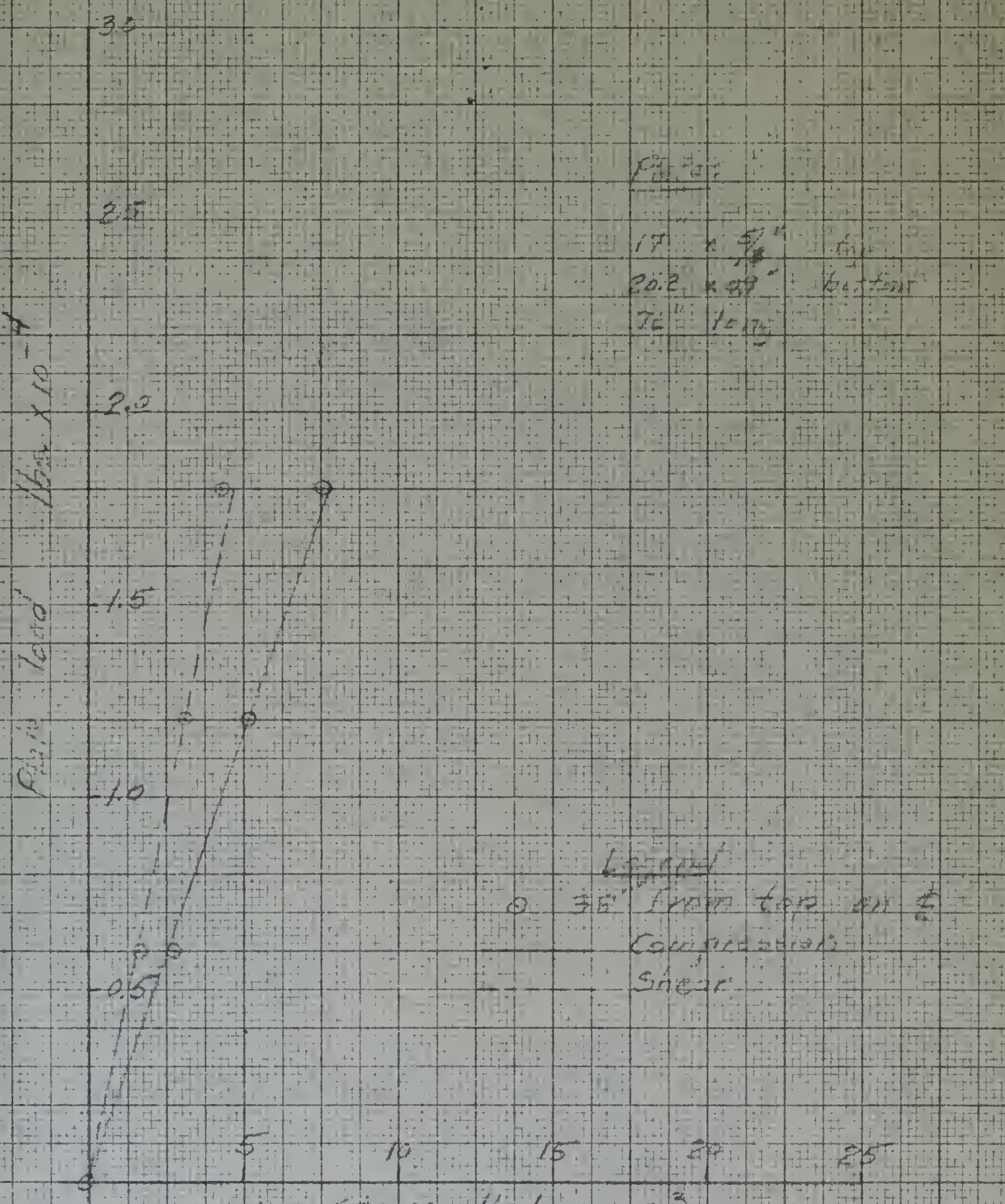

Fig 6

Plate Load vs. Max. Cover Sheet (E) Stress

(Test #1)

Ref. Table I

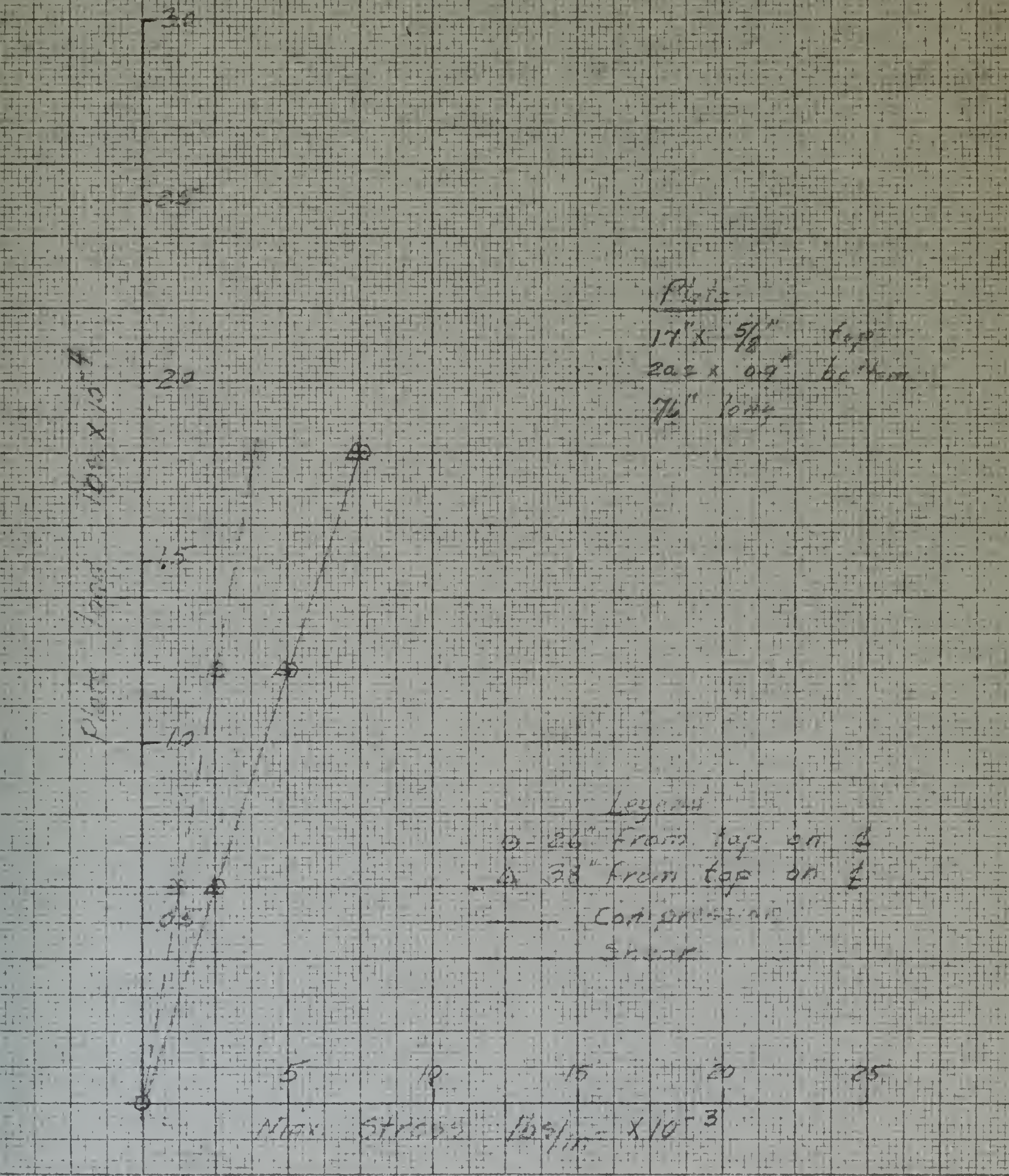

Fig. 7

Plate Load vs. Max Corrugation Stress
(Test #1)
Ref. Table I

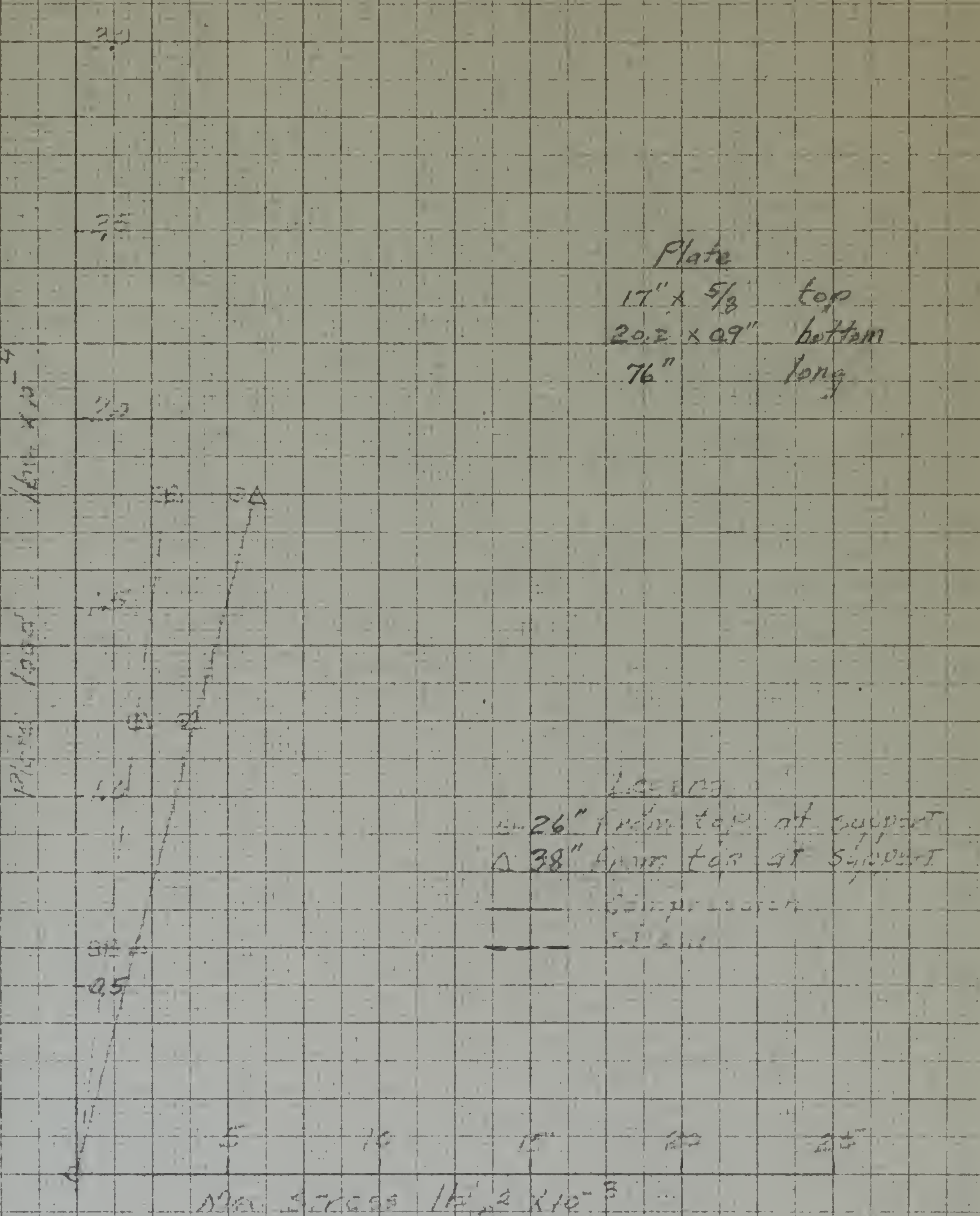

Fig 1

Plate Load vs. Wire Center sheet (1) Stress

(Test #2)

Ref Table II

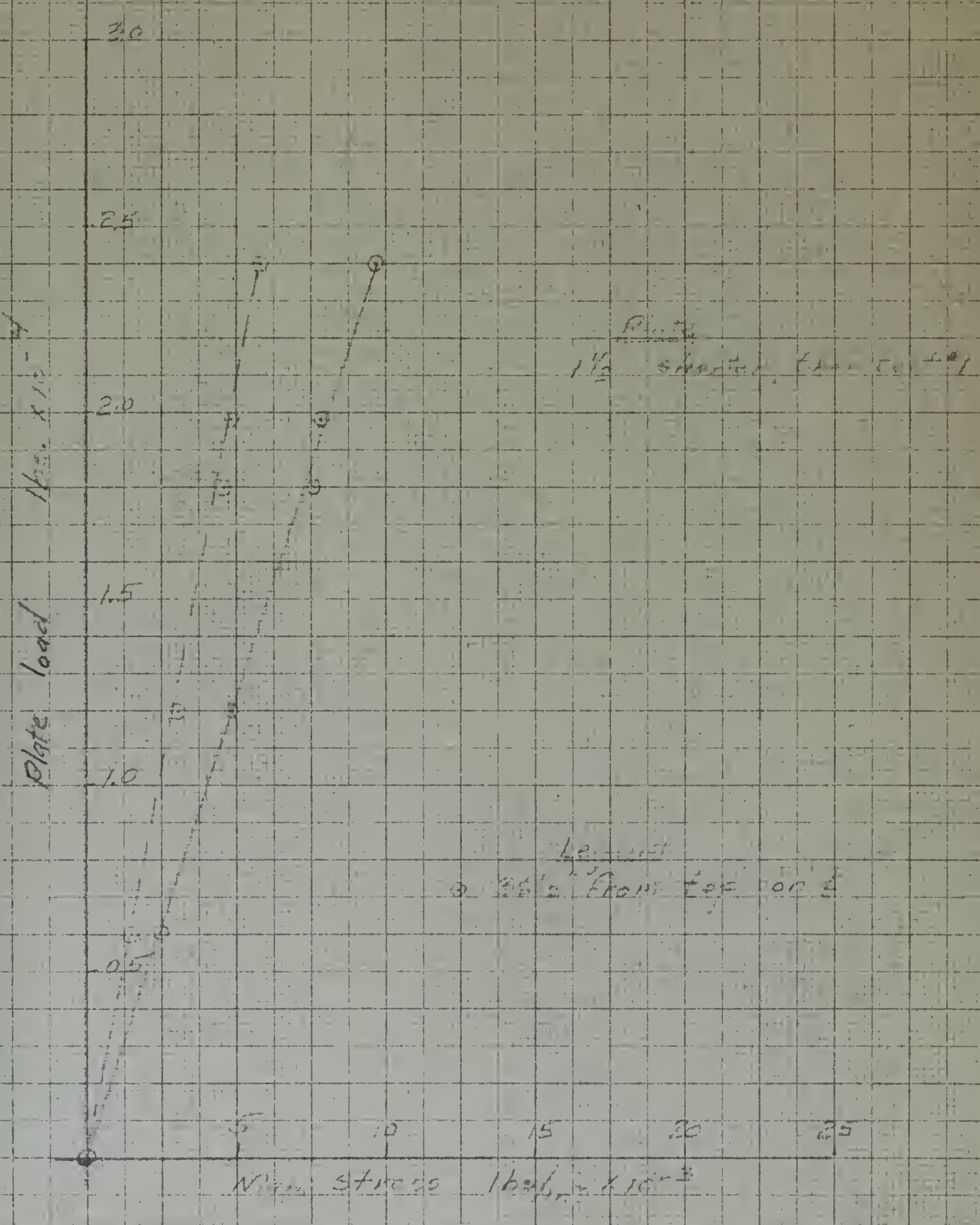

Fig. [illegible]

Plate Load vs. Max. Concentrated Stress

Test #2

Ref Table II

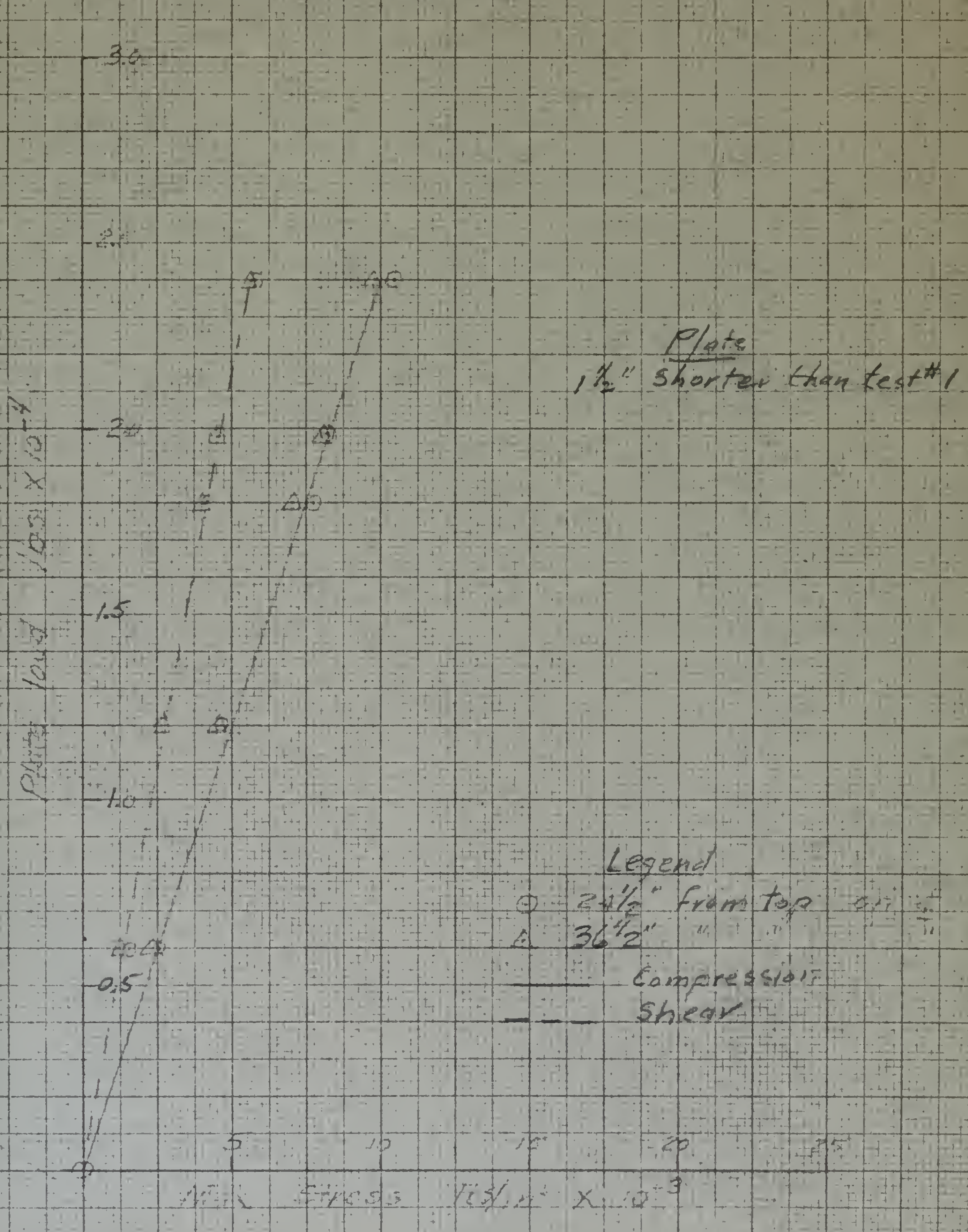

Fig. 10

Plate Load vs. Max. Corrugation Stress

(Test #2)

Ref. Table II

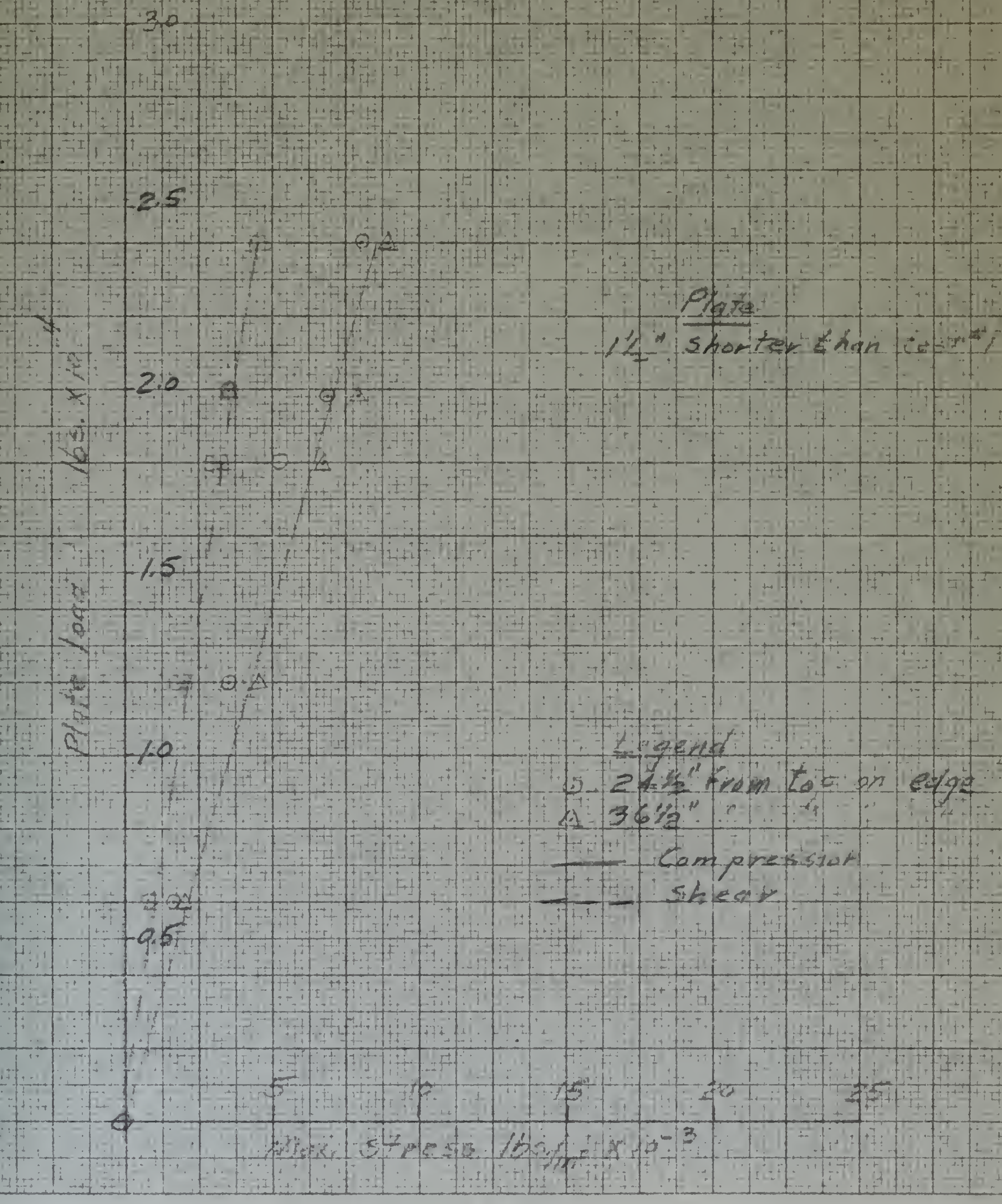

Fig. 11

Plate Load vs. Max. Cover Sheet (N) Stress

(Test #3 [illegible])

Ref Table IV

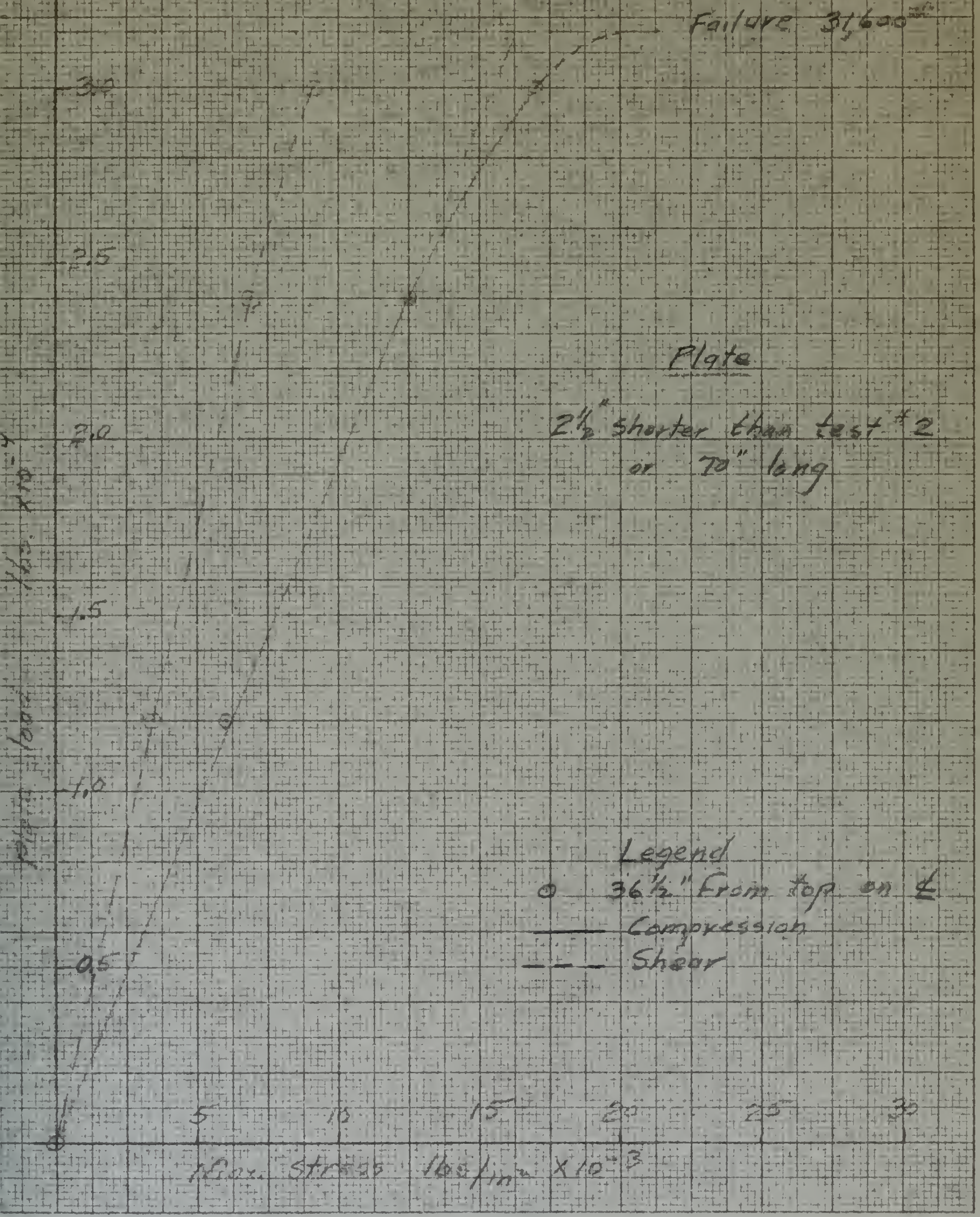

Fig. 12

Plate Load vs Max Cover Sheet (2) Stress
(Test #3 Destruction) Ref. Table III

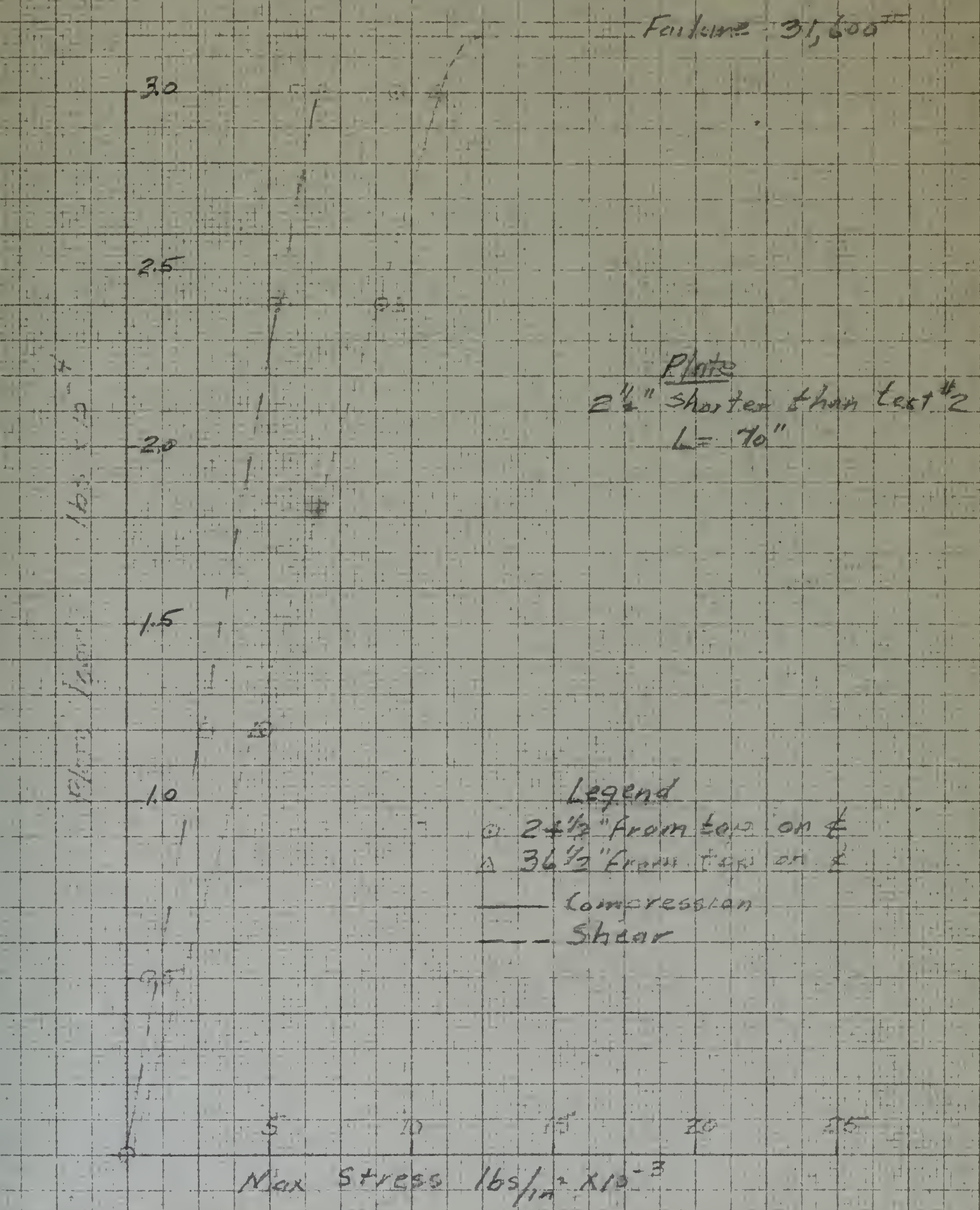

Fig. 13

Plate Load vs. Max Corrugation Stress

(Test #3) Ref Tab III

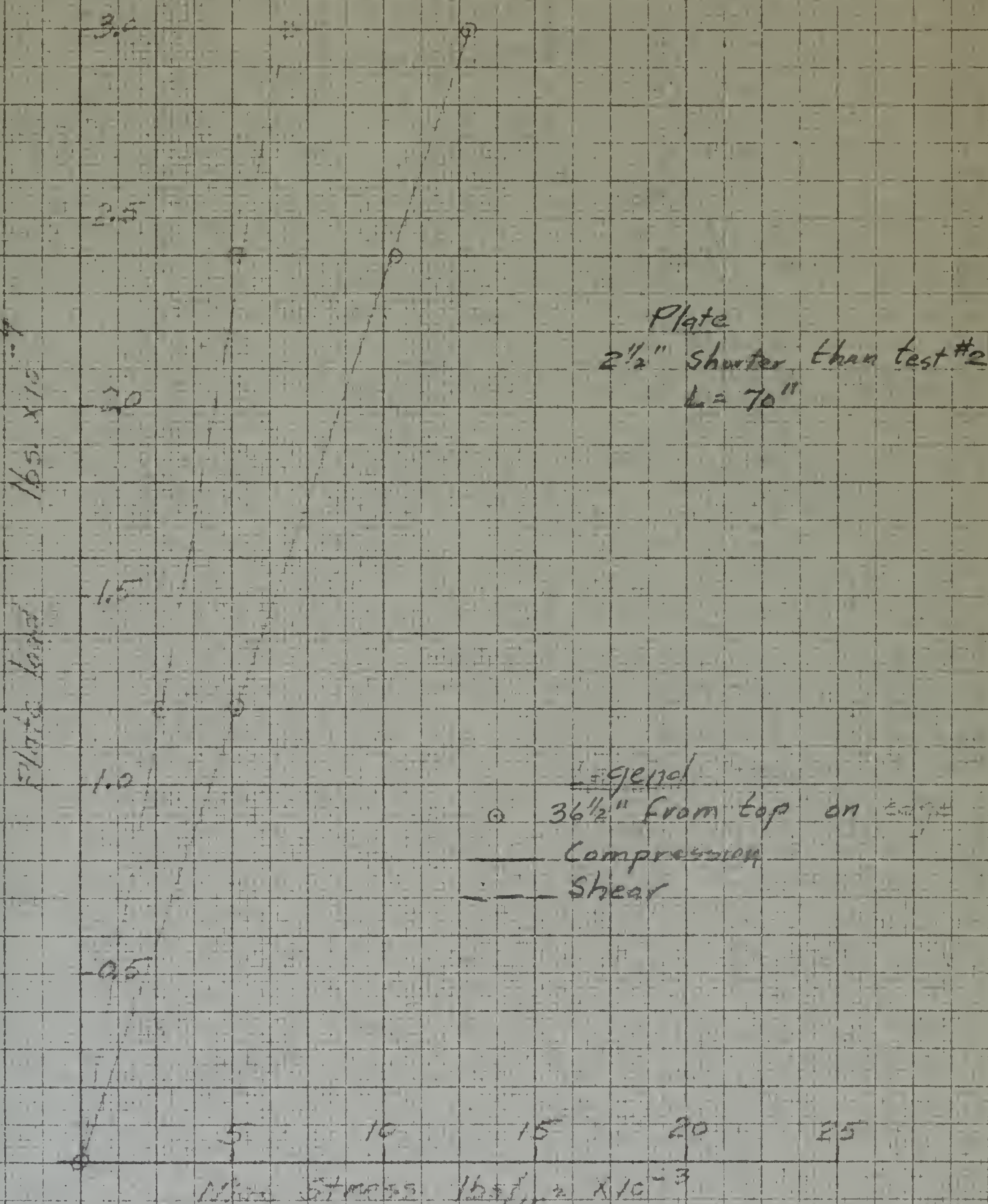

Fig. 14

Plate Load v.s. Maximum Stress
(Test # 4 Destruction)
Ref. Table IV

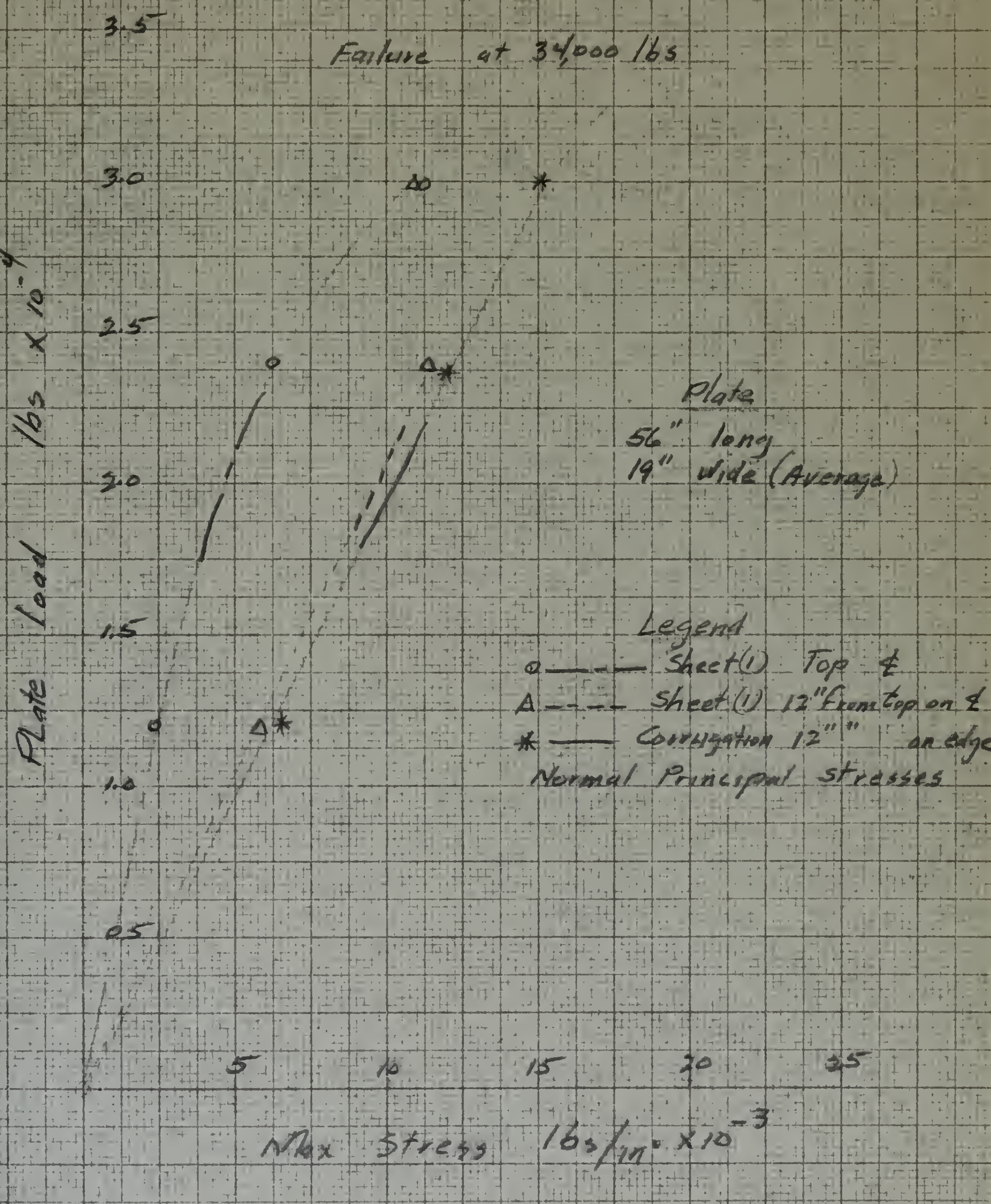

Fig. 15

Sheet and Corrugation
Properties
(Average Section)

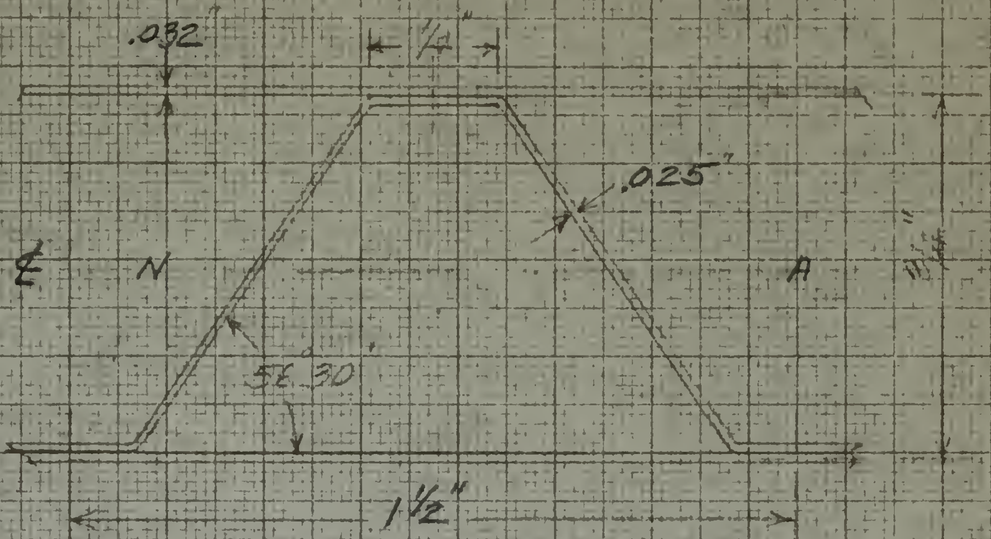

Sheet and corrugation joint
by 1/8" cherry rivets
on both sides

Properties

Sheet

$A = 0.064$ in.^{2}/in.
$I = 0.00765$ in.^{4}/in. {bare properties}
14 ST Alclad
$t_s = 0.0272$ bare

Corrugation

$A = 0.0357$ in.^{2}/in.
$I = 0.00245$ in.^{4}/in. {bare properties}
301-T Alclad
$t_c = 0.0222$ bare

Fig. 16
Sheet and Corrugation
Properties
(Minimum Section)

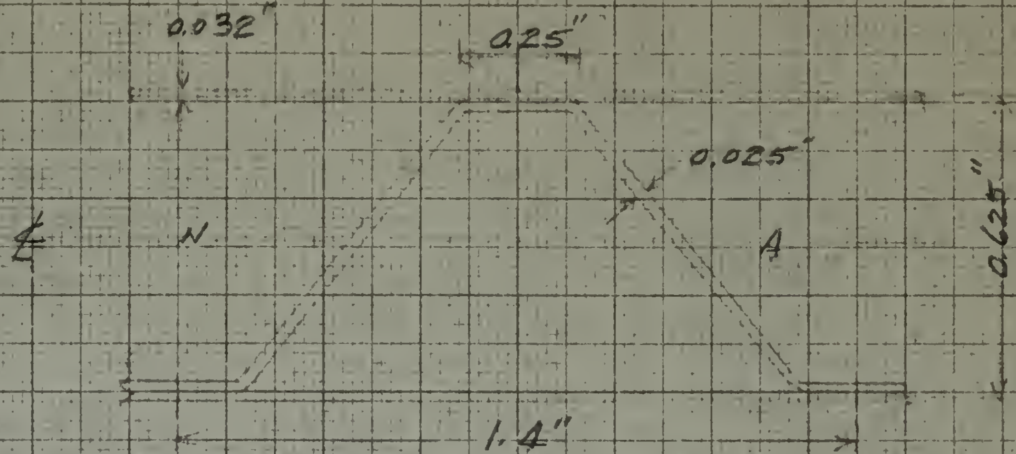

Sheet and Corrugation joined
by 1/8" Cherry Rivets
on both Sides

Properties

Sheet

$A = 0.064 \; in^2/in$
$I = 0.005475 \; in^4/in$ {bare properties}
$t_s = 0.0272$ in. bare
14 S-T Alclad

Corrugation

$A = 0.0375 \; in^2/in$
$I = 0.00159 \; in^4/in$
$t_c = 0.0222$ in. bare
301-T Alclad

Fig. 17

Compression Properties 301-T, 14S-T
Alclad sheet

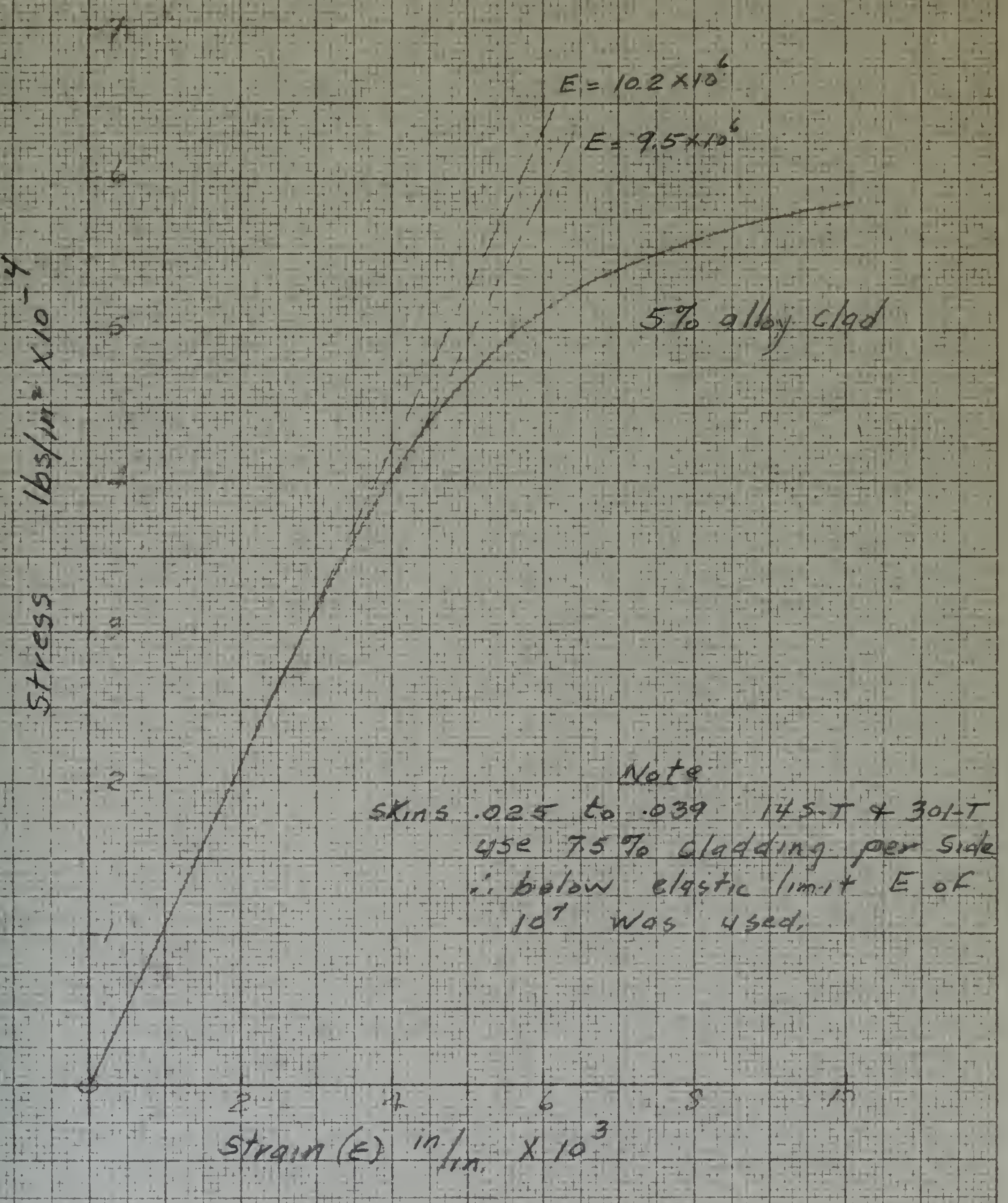

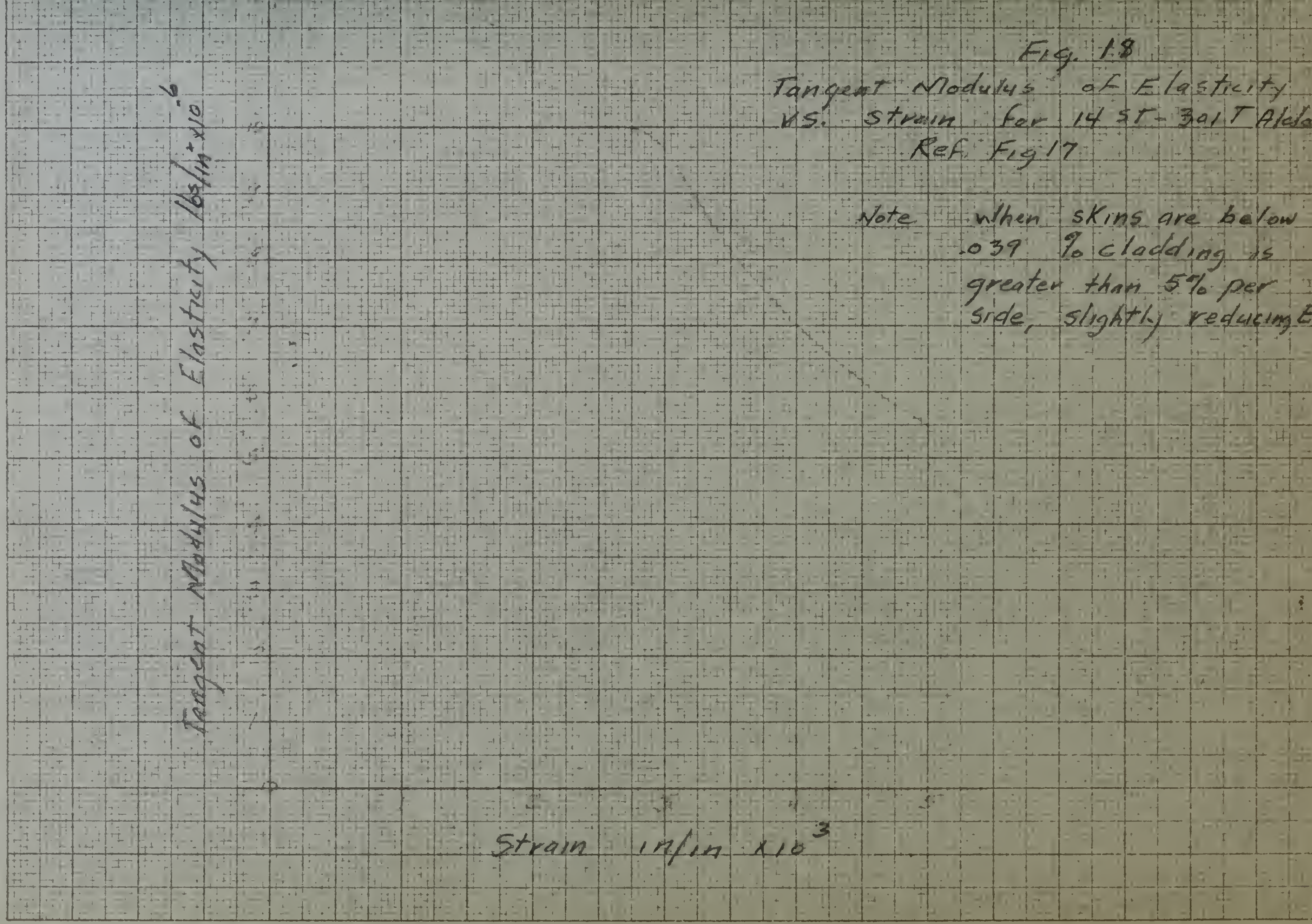

Fig. 18

Tangent Modulus of Elasticity VS. Strain for 14 ST-3a1 T Alclad

Ref. Fig 17

Note when skins are below .039 % cladding is greater than 5% per side, slightly reducing E.

Fig. 19
Average Stress of sheet vs. Strain beyond initial instability point of sheet

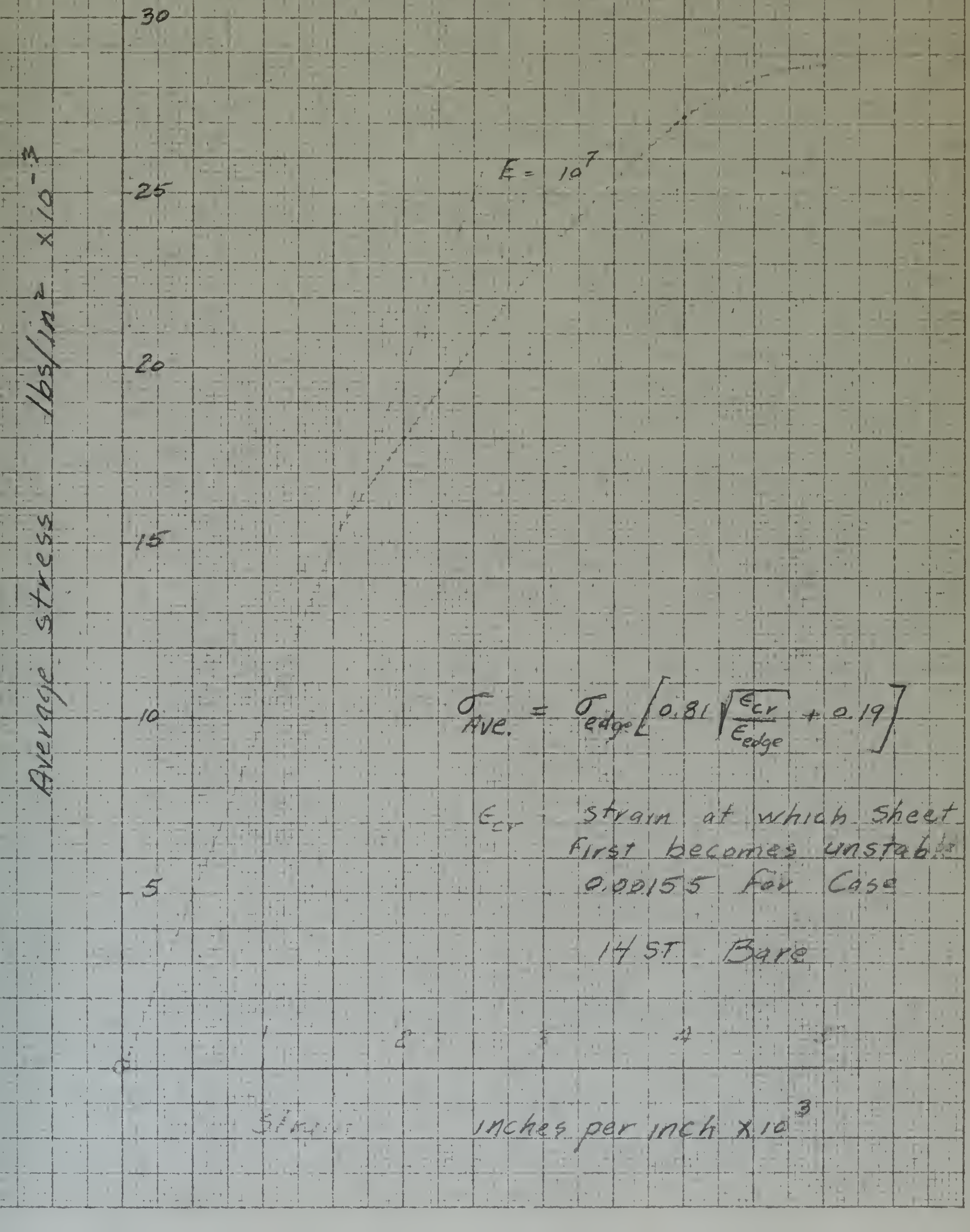

Fig. 20
Tangent Modulus of Elasticity
vs. Strain for 14 ST sheet
beyond initial instability point
(Ref. Fig. 19)

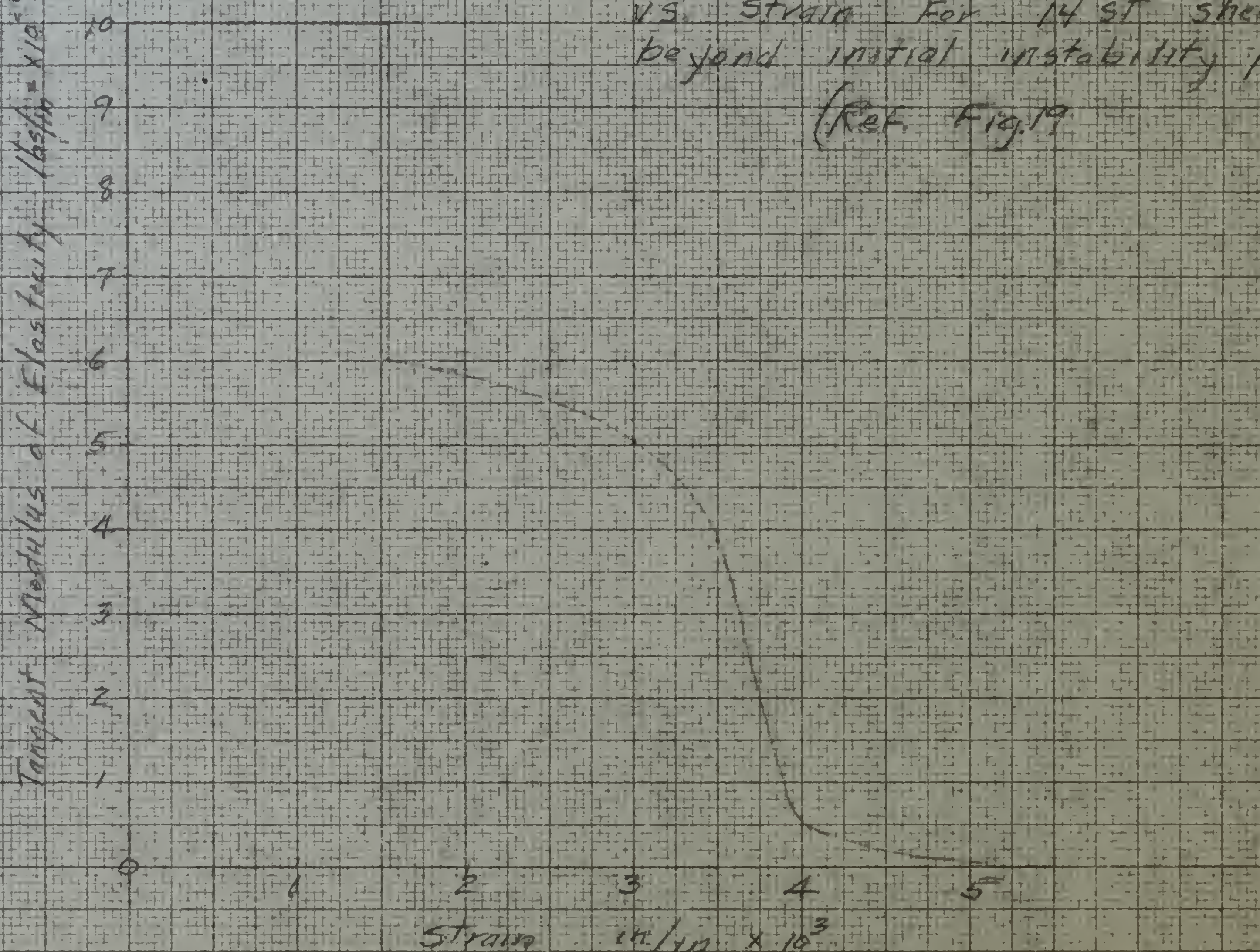

Fig. 21

Predicted Critical Plate Load